# Diffusion, elasticity, and shear flow in self-assembled block copolymers: A molecular dynamics study

Blair Fraser, Colin Denniston, and Martin H. Müser
Department of Applied Mathematics, University of Western Ontario, London, Canada, N6A 5B7

**Abstract.** Self-assembled ordered structures composed of block copolymers are simulated by molecular dynamics in stress-free conditions and under shear. We address several methodological points. The system must be allowed to adjust its size to accommodate natural periods of self-assembled structures. In addition, these structures need to be capable of rotating freely under shear. An examination of the diffusion of polymer molecules in the lamellar phase reveals sub-diffusion along translationally invariant directions between the ballistic and the diffusive regime. The diffused distance $d$ increases with time $t$ as $d \propto t^{1/3}$. We also examine the possibility of mapping structures such as cylindrical phases onto particle plus field types of models. By measurements of the $q$-dependent dynamical matrix, we show that this cannot be done using only two-body potentials. We then examine the molecular origin of shear alignment of lamella phases. Lamellae oriented parallel to the shear direction are seen to become unstable at high shear rates when the tensor of gyration of individual polymers form an average angle of 45° with the lamellae. This instability can be understood in analogy to similar transitions in liquid crystals.

# 1 Introduction

Computer simulations of polymer molecules are an important tool for studying their collective, macroscopic properties. Consequently, there is a large body of research using Monte-Carlo and also mean-field methods to study the equilibrium properties of such materials [1, 2]. However, while these approaches allow one to study large systems in reasonable amount of computational time, they generally do not allow the rigorous study of non-equilibrium properties. For this purpose, molecular dynamics can be a more appropriate method. Coarse-grained molecular dynamics in particular allows one to address some of the non-equilibrium properties without sacrificing too much in terms of computational speed [3, 4]. While there is a lot of established literature on the non-equilibrium dynamics of bulk [5, 6], confined [7, 8], or grafted polymers [9, 10], fewer simulations have been devoted to the rich non-equilibrium dynamics of self-assembled diblock copolymers. Only recently have some computational studies been reported, i.e., Refs. [11, 12, 13, 14, 15].

A diblock copolymer is a chain molecule composed of two covalently bonded sub-chains, one of which is composed of type $A$ monomers, and the other of which is composed of type $B$ monomers. Usually type $B$ monomers are chosen such that they resist mixing with type $A$ monomers. In a melt of such monomers, the immiscibility of $A$ and $B$ drives the system to phase separate into regular patterns of alternating $A$-rich and $B$-rich regions as the temperature is reduced below some critical temperature $T^*$. A wide variety of equilibrium micro-structures,

including lamellae, cylinders, and micellar fcc and bcc phases, appear below $T^*$ and have been the object of numerous experimental and theoretical works [16, 17].

The selection among the various equilibrium structures has been successfully modeled using self-consistent field theories which compare the free energy of a polymer chain in different potential structures to ascertain the minimum free energy structure [18, 19, 20, 21, 22]. The resulting phase diagram depends on two parameters, the composition of the polymers and the Flory-Huggins $\chi$ parameter. The composition of the polymer involves the relative lengths of the sub-chains of type $A$ and $B$ monomers, $f = N_A/N$ where $N$ is the degree of polymerization of the polymers (i.e. the total number of monomers of which the chain is composed). The $\chi$ parameter describes the incompatibility between type $A$ monomers and type $B$ monomers.

When diblock copolymer structures are subjected to shear, the lamellar, rod or micellar structures are forced to re-orient with respect to the symmetry-breaking shear flow [23, 24, 25]. The shear-aligned structures may be formed by simply reorienting the preexisting-existing equilibrium phase, or by inducing a morphological change in the melt akin to a phase transition. Processes of this kind are believed to be relevant in various technological applications in particular in polymer processing and in the production of self-assembled nanostructures. The scientific interest in sheared block copolymers is growing. Recent studies have been concerned with the motion of grain boundaries in micellar structures [26], large-amplitude oscillatory shear flow of diblock and triblock copolymers [27], and the morphology of copolymers under shear [28], to name a few examples.

Despite significant early work [29], models for the dynamics under shear, are much less developed than equilibrium theories. A number of new approaches have been attempted recently, including time-dependent Landau-Brazovskii theories [30, 31, 32, 33, 34] and dynamic density functional theory [28]. Another natural approach to modeling the self-organized structures is to use a strongly coarse-grained model in which the interaction between the structural components are modeled with two-body interactions [35]. Such models have been very successful in describing the elastic properties of colloidal systems [36] and the dynamics of such systems are easily simulated.

A difficulty in employing coarse-grained/mesoscopic models is two-fold. Essentially no studies have been done for microscopic models incorporating proper hydrodynamic interactions and eventual three-body forces, hence it is difficult to assess the underlying assumptions of such a theory. For example, simulations indicate that the effective viscosity $\eta$ of sheared self-assembled block copolymers is extremely rate dependent and non-monotonic [15], i.e., $\eta$ increases near the transition between different steady-state phases. Second, the parameters of the models need to be measured in order to make predictions (as opposed to generating self-consistent results). We will use molecular dynamics simulations to address some of these issues.

In the following section on methodology we outline the model and methodology we will use. While we mainly see this study as a feasibility study, we address an issue that does not come about in equilibrium simulations: The broken symmetry due to shear requires a more sophisticated treatment of the boundary conditions than it is the case for equilibrium. It is therefore necessary to allow the system to breath along the solid directions, while care has to be taken to allow fluid directions to adjust themselves. In the first part of the results section we examine the question of whether it is possible to parameterize the elastic response

of self-assembled rod in terms of two-body potentials between the rods. This will be done by calculating a suitably defined dynamical matrix for the system. In the last part of the result section, we examine the shear response of a lamella phase and investigate the molecular origin of shear alignment.

# 2 Methodology

## 2.1 MD Potentials

We use molecular dynamics to study melts of diblock-copolymers. By coarse graining long polymers so that one coarse-grained monomer represents one persistence length of a long polymer chain, a bead-spring model where the beads interact through a spherically symmetric potential can be used [3]. To provide excluded volume effects, the monomers have a repulsive hard core, for which one typically uses a truncated and shifted Lennard-Jones potential, i.e., $U_{ij}(r) = 4\epsilon_{ij}\left[(\sigma/r)^{12} - (\sigma/r)^{6} + 1/4\right]$ for $r \leq r_c$ and $U_{ij}(r) = 0$ for $r > r_c$. Here $r$ is the distance between particles $i$ and $j$, $r_c = 2^{1/6}\sigma$ is the interaction cutoff distance and $\epsilon$ and $\sigma$ control the energy and length scales respectively.

In order to induce the system to phase separate, a bias must be introduced into the potential. The bias is often introduced through the leading parameter $\epsilon_{ij}$ by setting $\epsilon_{AA} = \epsilon_{BB} < \epsilon_{AB}$, thus increasing the repulsion between unlike monomers. Because short polymers require a stronger bias before one sees phase separation, it is often insufficient to use $\epsilon_{ij}$ for the bias parameter. However, we can also introduce the bias by adding a short range attractive well between like monomers and leaving $\epsilon$ constant for all interactions [4]. With this choice of potential we can study phase separation in chain polymers as short as two monomers in length. Using the attractive well has the additional advantage of allowing us fine control of the interaction radius relative to the hard core radius, which we keep very short for computational reasons. Following [4] we use the potential,

$$U_{ij}(r) = \begin{cases} 4\epsilon\left[\left(\frac{\sigma}{r}\right)^{12} - \left(\frac{\sigma}{r}\right)^{6} + \frac{1}{4}\right] - \gamma_{ij}, & r \leq r_c \\ \frac{1}{2}\gamma_{ij}\left[\cos(\alpha r^2 - \beta) - 1\right], & r_c < r \leq R_c \\ 0, & r > R_c \end{cases} \tag{1}$$

The constant $\gamma_{ij}$ sets the depth of the potential well at $r_c$ ($\gamma_{ij} = 0$ if monomers $i$ and $j$ are of different species, and $\gamma_{ij} = \gamma$ if they are of similar species). We also take $\epsilon = \sigma = 1$, and

$$\begin{aligned} \alpha &= \frac{4\pi}{9 - 2^{\frac{7}{3}}}, \\ \beta &= \frac{\pi\left(9 - 2^{\frac{10}{3}}\right)}{9 - 2^{\frac{7}{3}}} \end{aligned} \tag{2}$$

are chosen to make the potential continuous and smooth.

The monomers are chained together using the anharmonic FENE ("finitely extensible non-linear elastic") potential,

$$U^{ch}(r) = \begin{cases} -\frac{1}{2}kR_0^2 \ln\left[1 - \left(\frac{r}{R_0}\right)^2\right], & r \leq R_0 \\ \infty, & r > R_0 \end{cases} \tag{3}$$

in which $R_0$ is set such that unphysical chain crossings are disallowed at the simulation temperature [3]. At $T = 1$, we use $R_0 = 1.5\sigma$ and $k = 30\epsilon\sigma^2$.

The equations of motion are integrated with a standard velocity-Verlet algorithm with a time-step of 0.01 [37]. The simulation sizes we are dealing with range from 5000 monomers to 20 000 monomers, simulated for times of $10\,000\tau$ to $20\,000\tau$.

## 2.2 Imposing temperature and shear

As we will be applying shear later in this paper, the choice of thermostat is an important one. We use a DPD thermostat, which thermostats on the center of mass of interacting particles [38].

The DPD equations of motion are given by

$$\dot{\mathbf{r}}_i = \frac{\mathbf{p}_i}{m_i}, \tag{4}$$

$$\dot{\mathbf{p}}_i = \mathbf{F}_i + \mathbf{F}_i^{\mathbf{D}} + \mathbf{F}_i^{\mathbf{R}} \tag{5}$$

where $\mathbf{F}_i^{\mathbf{D}}$ and $\mathbf{F}_i^{\mathbf{R}}$ are additional damping and random noise forces acting on particle $i$. These additional forces are in turn based on the sum of forces at the center of masses of interacting particles of which $i$ is a partner.

$$\mathbf{F}_i^{\mathbf{D}} = \sum_{j \neq i} \mathbf{F}_{ij}^{\mathbf{D}}, \tag{6}$$

$$\mathbf{F}_i^{\mathbf{R}} = \sum_{j \neq i} \mathbf{F}_{ij}^{\mathbf{R}}, \tag{7}$$

If we define the interatomic distance $\mathbf{r}_{ij} = \mathbf{r}_i - \mathbf{r}_j$ and the relative velocity $\mathbf{v}_{ij} = \mathbf{v}_i - \mathbf{v}_j$ we can express $\mathbf{F}_i^{\mathbf{D}}$ and $\mathbf{F}_i^{\mathbf{R}}$ as

$$\begin{aligned} \mathbf{F}_{ij}^{\mathbf{D}} &= -\zeta w^D(\mathbf{r}_{ij})\,(\mathbf{r}_{ij} \cdot \mathbf{v}_{ij})\,\mathbf{r}_{ij}, \\ \mathbf{F}_{ij}^{\mathbf{R}} &= \sigma w^R(\mathbf{r}_{ij}) \Gamma_{ij} \mathbf{r}_{ij}. \end{aligned} \tag{8}$$

where $\zeta$ is a friction constant, $w^D(r)$ and $w^R(r)$ are weight functions, and $\sigma$ is the noise strength. $\Gamma$ is a white noise variable whose distribution satisfies

$$\begin{aligned} \langle \Gamma_{ij}(t) \rangle &= 0, \\ \langle \Gamma_{ij}(t) \Gamma_{kl}(t') \rangle &= (\delta_{ik}\delta_{jl} + \delta_{il}\delta_{jk})\delta(t - t'). \end{aligned} \tag{9}$$

To satisfy the fluctuation-dissipation theorem, we also require that

$$\begin{aligned} \sigma^2 &= 2k_B T \zeta, \\ \left[w^R(r)\right]^2 &= w^D(r). \end{aligned} \tag{10}$$

We choose the weight functions as

$$w^D(r) = w^R(r) = \begin{cases} 1, & r < R_c \\ 0, & r \geq R_c \end{cases} . \tag{11}$$

The DPD thermostat has some distinct advantages over other methods of thermostatting. Because the DPD thermostats on the center of mass of interacting particles, it conserves momentum both locally and globally. This is in contrast to a Langevin type thermostat which thermostats on the absolute velocity of a monomer, thus damping hydrodynamic flow. When simulating under shear, the DPD thermostat will not dampen the flow in the long wavelength limit that we have imposed on the system. Also, DPD does not impose a preferred velocity profile in the simulation cell, which may be an undesired side effect of Gaussian or other thermostats. However, the DPD thermostat is a slower algorithm computationally than the Langevin thermostat, requiring the thermostatting on every interaction between monomers at every time step. This can be alleviated somewhat by thermostatting on randomly chosen time steps. We thermostat, on average, only every other step. This change does not affect results in a significant manner.

When diblock copolymer melts are subjected to shear flow, many phases, such as the lamellar or cylindrical phase, are forced to realign with the shear direction. Additionally, it has been found experimentally that shear is a useful tool to align a large sample of the lamellar phase in a single direction. When large films of diblock copolymers are relaxed to the lamellar phase in equilibrium, they often relax into grains, where within each grain, the lamellae are well aligned, but at grain boundaries the lamellae do not match up well. It would take an exceedingly long time for the grains to reorient their lamellae to their neighboring grains. However, when the same system is relaxed under periodic shear flow, the lamellae are only able to form in a shear-aligned direction, thus producing a large sample of perfectly aligned lamellae. To impose shear flow on our molecular dynamics simulation, we use Lees-Edwards boundary conditions [39]. In this scheme, each monomer in the simulation feels a neighboring monomer not from its actual position, but from a position offset by a distance $\delta(t, z)$ in the direction of shear flow and dependent on the shear normal $z$.

## 2.3 Barostat and box geometry

In segregated melts of diblock copolymers, each of the polymers are likely to be found with their $A$ and $B$ ends embedded in regions composed of high concentrations of like monomers. When the system assembles into a regular structure, such as the lamellar or cylindrical phase, these domains have a preferred size and spacing, partially determined by the degree of polymerization and the temperature. The result of this preferred spacing is that the assembled structures behave as a solid along periodic (or quasi-periodic) directions, while they behave as a fluid along translationally invariant directions. For example, the disordered phase has three fluid directions, there are no significant barriers to diffusion in any direction above the glass transition temperature. However, the lamellar phase has one solid direction, (perpendicular to the lamellae), and two fluid directions, as indicated in Fig. 1. The other phases can be considered in a similar manner. The cylindrical phase has two solid directions perpendicular to

the cylinders, and one fluid direction along they cylinders, while fcc and bcc phases have three solid directions.

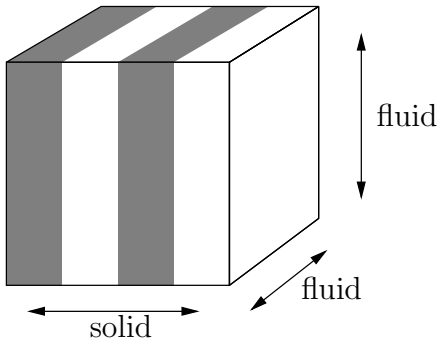


Figure 1: The lamellar phase has a preferred spacing in the direction perpendicular to the lamellae. This gives it solid-like properties in this direction while flow properties along the other two directions remain fluid like.

Each of the periodic structures that diblock copolymers form in equilibrium have a preferred period, thus giving an integral number of periods a preferred length. While it might be suitable to constrain the width of the simulation box in equilibrium such that the natural spacing of lamellae or rods is satisfied [40], non-equilibrium situations are likely to require a more sophisticated approach. The simulation box should ideally be allowed to fluctuate at least in each of the solid directions to enable the system to find its natural spacing. Thus the size of the simulation box in each solid direction should be controlled by imposing an external pressure on the walls of the box in this direction.

We have the option however, (i) to allow the length of the simulation box in the liquid directions to vary (isotropically) based on a constant external pressure, or (ii) to impose a constant volume of the simulation box and vary the remaining direction(s) this way. However, one has to keep in mind that one cannot allow fluid directions to fluctuate or to adjust independently from the other fluid directions. That is, they must be constrained by the same external pressure for option (i), or constrained so that their lengths have a fixed ratio for option (ii). Otherwise, it is possible (and likely) that the simulation box gets squeezed into a flat, effectively two-dimensional structure.

Allowing the box geometry to vary independently along certain directions in response to an imposed external stress simulation will introduce some complicating issues into a diblock copolymer simulation. For example, if the external pressure is greater than the indentation hardness of the system, then the system can collapse just again into a quasi two-dimensional structure. In simulations, this may often be the case, when for reasons of computational efficiency, short cut-off radii are chosen that are compensated effectively by a positive external pressure.

The phases we are focusing on in this study are lamellae or rod structures. These fit into an orthorhombic simulation cell. Therefore, it is sufficient to vary the simulation cell within orthorhombic geometries. When the system is sheared, this is not done by expressing

the geometry explicitly as monoclinic, but rather through imposing Lee-Edwards boundary conditions as discussed above.

# 3 Results

The bias parameter $\gamma$ in the model potential Eq. (1), acts like an inverse temperature with respect to the phase transition. That is, for a melt of diblock copolymers at equilibrium in the disordered phase, we can induce a phase transition either by decreasing the temperature below some temperature $T^*$, or by increasing the bias parameter. Much as we had a $T^*$, we also have for fixed temperature a $\gamma^*$. In lieu of reducing the temperature to drive the phase transition, we have chosen to use $\gamma$. We first estimate the value of $\gamma$ that will lead the system to phase separate.

Using symmetric diblock copolymers of chain length $N = 10$, we find that a melt at a constant density of 0.85 and at a constant temperature of 1.0 will phase separate into a lamellar structure for values of $\gamma$ greater than about 1.0. The simulation time it takes to order into a lamellar structure from an initially disordered phase is reasonable ($\sim 10\,000\tau$) for values of $\gamma$ greater than about 1.2. We use $\gamma = 1.3$ for all of our simulations.

## 3.1 Diffusion

The consequences of solid and fluid directions are borne out in the anisotropy of polymer diffusion [40, 41, 42, 43]. While most studies appear to focus on the order-disorder transition region, the anisotropy becomes particularly strong at smaller temperatures. There are high activation barriers preventing the ends of the polymers from moving between two non-contiguous regions of like monomers within reasonable times, however, a polymer can diffuse relatively easily within a lamella along the translationally invariant directions. Figure 2 shows a graph of the diffusion in the $x$, $y$ and $z$ directions, where the $z$ direction is perpendicular to the lamellae. Diffusion in what we have called the solid direction levels off at or below the width of the lamellae, while in the liquid directions it increases linearly at large times as it should in a liquid. Of course, at extremely large time scales, polymers will diffuse between different lamellae, rods, or micelles but there is a well-defined time scale separation between this process and most other processes so that this migration can be neglected for our purposes here.

In Fig. 2, it is possible to identify an extended region in which the average distance traveled $d$ increases as a $t^{1/3}$ power law. No theories are known to us that predict this type of sub-diffusive regime. Moreover, experimental data has not yet been presented in a way that would allow one to obtain $d(t)$ in a straight forward way. Most simulations appear to be too close to the disorder transition so that sub-diffusion cannot appear. At this point, we have not done studies investigating whether there are reasons to believe that this behavior can be found universally within certain temperature regimes.

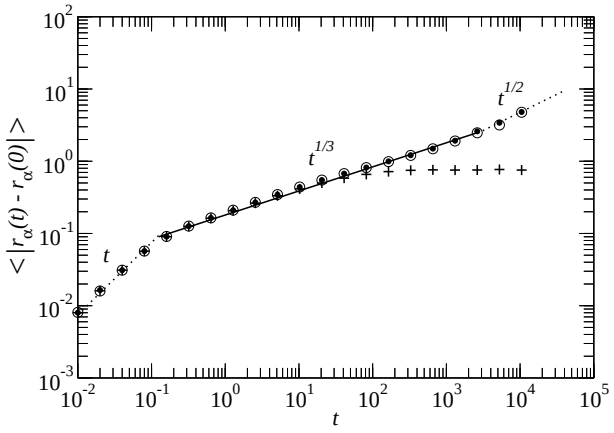


Figure 2: Diffusion of monomers, $\langle |r_\alpha(t) - r_\alpha(0)| \rangle$ for $\alpha \in \{x, y, z\}$, as a function of time in a lamella system with lamella oriented perpendicular to the $y$-direction. The lines are drawn to guide the eye. They represent the power laws indicated in the figure. Details of the simulations are: $T = 1$, depth of adhesive well $\gamma = 1.3$, and external (average) pressure $p = 5$.

## 3.2 Elastic response

As the composition of the monomers is changed, we see some of the rich phase diagram that diblock-copolymers produce. Changing the composition of the polymers from $N_A = 5$, $N_B = 5$ to $N_A = 7$, $N_B = 3$ we see that the polymers relax into a cylindrical phase, like that shown in Fig. 3(a). This phase is predicted theoretically and seen experimentally where cylinders extending in what we have labeled the $z$ direction arrange themselves in a trigonal lattice in the $x - y$ plane.

The trigonal arrangement of the cylinders resembles that of some adsorbed two-dimensional atomic solids such as a trigonal layer of helium on graphite. Once such a periodic structure is given, it is natural to address small fluctuations of the relevant degrees of freedom around the reference structure. For the rods shown in Fig. 3, this can be done in analogy to small-amplitude oscillations of atoms in crystals. Metaphorically, one could associate the position of a helium atom with the center of mass of a rod. What usually are the internal, electronic degrees of freedom are now the monomers attributed to a rod. These include the monomers that are covalently attached to those 'central' monomers.

Given this analogy, (the center of masses of) the rods move on free energy potential surfaces. Note that (in a classical system) no time-scale separation of the rod degrees of freedom and the monomer degrees of freedom needs to be given so that we can define a meaningful free energy for the interaction between rods. Similar to interatomic potentials, it should be possible to expand the free-energy surface $\mathcal{F}$ into two-body, three-body, and higher-order terms. Here, we want to address the question whether it would make sense to truncate the expansion after the two-body term. Due to the short range of the interaction potential, only neighboring rods touch directly. We therefore only need to take into account interactions between nearest neighbors.

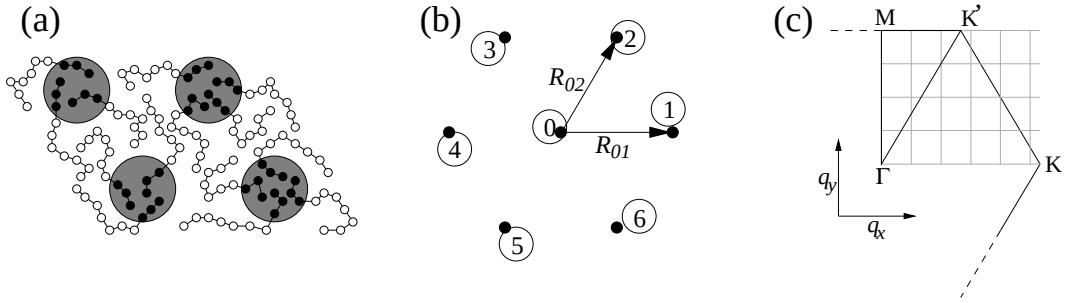


Figure 3: (a) Cartoon of the cylindrical phase. The shorter A-type part of the polymer chains (shown in black) organize into cylinders leaving the space in between to be filled by the B-type part of the polymers (shown in white). (b) Nearest neighbors of a central rod in trigonal phase. White dots indicate the ideal positions and the number of the atom, black dots indicate an instantaneous position. (c) Path in reciprocal space along which the dynamical matrix will be measured further below. Vertices of the lattice indicate wave vectors $\mathbf{q}$ commensurate with the periodic boundary conditions. They are the only points that can be measured. For the evaluation of the branches MK$^*$ and $K\Gamma$, we evaluated symmetrically equivalent phonons on the $\Gamma K$ axis.

Thus, in this approximation, the full elasticity of the trigonal lattice is described by one single parameter $k$, which describes the curvature of the two-body potential in its minimum. In this sense, if $a$ is the preferred spacing between the atoms, one can expand the free energy between the rods into:

$$\mathcal{F} = \mathcal{F}_0 + \frac{1}{2}k\sum_{j=1}^{6}\left[\sqrt{(X_0 - X_j)^2 + (Y_0 - Y_j)^2} - a\right]^2, \tag{12}$$

where $\mathcal{F}_0$ is the (presently irrelevant) free-energy for a perfectly trigonal configuration and $X_j$ and $Y_j$ are the coordinates of the rods in the plane orthogonal to the rods. The sum in Eq. (12) runs over all neighbors, see also Fig. 3(b). As we only assume zero pressure and small amplitude motion, we may associate $a$ with the average nearest-neighbor spacing.

Following standard textbook treatments, we then express the free energy in reciprocal space. One can associate the free energy $\mathcal{F}(\mathbf{q})$

$$\mathcal{F}(\mathbf{q}) = \frac{1}{2}D_\alpha^\beta(\mathbf{q})u_\alpha(\mathbf{q})u_\beta(\mathbf{q}) \tag{13}$$

with a mode (or two modes) $\mathbf{u}(\mathbf{q})$ associated with wave vector $\mathbf{q}$. Here we have introduced (except for a factor of unit mass) the dynamical matrix $D_{\alpha\beta}$:

$$D_\alpha^\beta(\mathbf{q}) = 2\sum_j \frac{\partial^2\mathcal{F}_{0,j}}{\partial R_{0,\alpha}\partial R_{0,\beta}}\sin^2\left(\mathbf{q}\mathbf{R}_{0j}/2\right), \tag{14}$$

where $\mathcal{F}_{0,j}$ represents the two-body interactions that appear on the right-hand side of Eq. (12), $R_{0,\alpha}$ is the $\alpha$ component of the rod number zero, and all derivatives are evaluated at the

reference structure. For the present problem, the result is:

$$\frac{1}{k}\,D(\mathbf{q}) = 4\sin^2(q_x a)\begin{bmatrix} 1 & 0 \\ 0 & 0 \end{bmatrix} + \sin^2(q_x a/2 + \sqrt{3}q_y a/2)\begin{bmatrix} 1 & \sqrt{3} \\ \sqrt{3} & 3 \end{bmatrix} + \sin^2(q_x a/2 - \sqrt{3}q_y a/2)\begin{bmatrix} 1 & -\sqrt{3} \\ -\sqrt{3} & 3 \end{bmatrix}. \quad (15)$$

It is now helpful to note that there is a unique and simple relation between the dynamical matrix and the thermal correlation of the Fourier transforms of the displacements $\langle u_\alpha(\mathbf{q})u_\beta(\mathbf{q})\rangle$ in the harmonic approximation, namely

$$\langle u_\alpha(\mathbf{q})u_\beta(\mathbf{q})\rangle = k_B T\left(D^{-1}(\mathbf{q})\right)_{\alpha\beta}. \quad (16)$$

This equation does not require the interactions be sums of two-body potentials but only the harmonic approximation to hold. Eq. (16) holds because the $u_\alpha(\mathbf{q})$ can be interpreted as Gaussian random variables. It is not necessary either that the cylindrical phase we are using be the equilibrium phase for what we are trying to do. The system only needs to be in a local energy minimum and stable for the time being studied.

We can now determine the *true* dynamical matrix $D$ (to be precise the Fourier transform of the force constants) by monitoring the rod fluctuations and fit the results to Eq. (15), which relied on assuming two-body interactions. In a similar way, long wavelength elastic constants have been determined by observing fluctuations of strains in two-dimensional systems composed of hard disks [44]. Here we perform an equivalent analysis, however, the full Brillouin zone is covered.

Before presenting the results, we wish to discuss possible origins for the discrepancy between the simulations and a two-body approach. For large temperatures one may expect anharmonic contributions. These, however, can certainly be neglected if the oscillations are less than 4% of the lattice constant, which is the case in our simulations presented below ($p = 0$, $T/\gamma = 0.346$). Besides the thermal fluctuations of the rods' centers of mass, there may be large *local* fluctuations, i.e., if we take a slice through the system at constant $z$ instead of averaging the positions over the full lengths of the rods. The extra dimension in $z$ direction can be seen in analogy to the imaginary time axis used in path-integral treatments of quantum-mechanical systems. Indeed non-thermal quantum fluctuations in quantum solids can be sufficiently strong to significantly break the Cauchy symmetry relations of the elastic constants which would be present in a classical treatment. Examples are the trigonal phases of helium adsorbed on graphite [45] and bulk solid helium [46]. However, for the analysis of three-body terms, we will focus our analysis on very short rods and can thus rule out this effect as well.

There may also be size fluctuations of the rods, which have been observed in more general circumstances, i.e., if large local pressures are present, polymers diffuse away from their rods to nucleate new ones [47]. In such circumstances, effective interactions would be an oversimplification, unless one were to include in the description additional internal degrees of freedom controlling the size of individual rods. In the present study, however, external conditions are isotropic, all cylinders are of equal size (on average) and diffusion of polymers between the cylinders is frozen out on the time scale of the simulation.

The last candidate for making a many-body description necessary is what we call the foam ball effect. While the time average cross section of each cylinder remains roughly circular, each cylinder can deform somewhat if it is pushed by neighboring cylinders. This deformation could in turn exert a force on a third cylinder. The mechanism is illustrated in Figure 4.

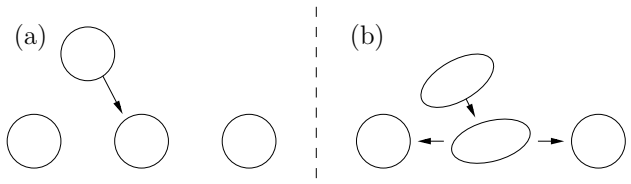


Figure 4: (a) Top view of four rods in their unperturbed circular shape. (b) One rod is moved and touches a secondary rod. Even if the secondary rod is confined to its position, it can deform and thus exert forces on tertiary rods.

Since one can probably rule out all other possible reasons, we believe that the foam ball effect will be mainly responsible for the leading-order corrections to an effective two-body behavior. A promising route to describe these corrections phenomenologically may well be to introduce additional internal degrees of freedom of the rods that describe the deviation between a circular rod and a deformed rod. Such an approach could account effectively not only for two-body interactions but for higher-order interactions as well. However, it is beyond the scope of this paper to develop new potentials incorporating the foam-ball effect. Our results will therefore only be a measure for the need to include higher-order terms.

In Fig. 5, we show the square roots $\omega$ of the eigenvalues of the dynamical matrix. There is a significant discrepancy between the best-possible fit assuming two-body potentials and the actually observed behavior. This also holds for the long-wavelength limit $\mathbf{q} \to 0$. The ratio $r$ of the 'frequencies' related to the longitudinal and transverse mode is $\sqrt{3}$ in the stress-free, two-body approach, which can be derived from Eq. (15). The rod cylinders show a ratio of $r \approx 4.5$ in the limit $\mathbf{q} \to 0$. While the shape of the longitudinal branch is at least close to that corresponding to central two-body interactions, the transverse branch differs qualitatively. One may thus expect that reliable effective theories of interactions between rods have to include many-rod interactions.

We will now comment on the details of the simulations leading to Fig. 5. To enable the simulation of a system spanning a large number of lattice constants (and to avoid the "quantum effects" discussed above), we examined fairly thin systems. However, making the system too thin decreases the barriers to cylinders breaking up and/or merging. The phonon spectrum and elastic constants are very temperature sensitive. In our simulations we have chosen the highest temperature for which we can simulate the cylinders for long times without breaking up or merging of cylinders. At $k_B T = 0.45\epsilon$ merging or breaking of the cylinders is rare, even in thin films.

Equilibration of large systems of polymers from random initial conditions is prohibitively expensive, we therefore had to start from a constructed initial condition. This was done by

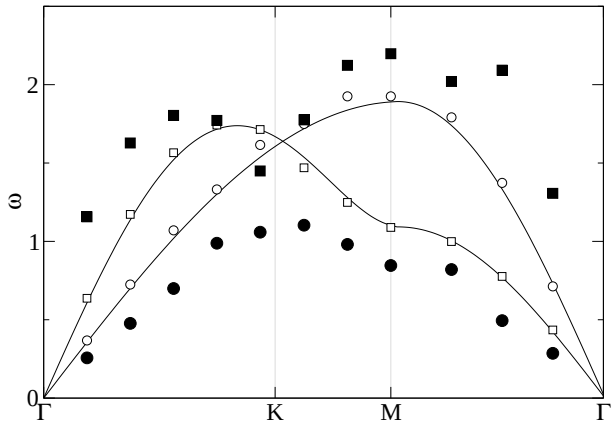


Figure 5: Square roots $\omega$ of the eigenvalues of the dynamical matrix at the wave vectors indicated in Fig. 3. The solid symbols correspond to the measurement of the diblock copolymer system in the cylindrical phase via Eq. (16) and their statistical error bars is symbol size. The data are scaled so that they have the same mean values as an ideal two-body system with $k = 1$, see Eq. (15) which is represented by the lines. The solid (dashed) line corresponds to the exact expression for the transverse (longitudinal) modes. The open symbols refer to a measurement of a test molecular dynamics system with interparticle potential exactly that of Eq. (12). The test runs have statistical errors slightly smaller than symbol size. Details of the simulation are: $\gamma = 1.3$, $T = 0.4$, and external pressure $p = 0$.

first performing several smaller runs with polymers composed of $N_A = 7$, $N_B = 3$. When equilibrated from random initial conditions, these polymers form a cylindrical phase. These systems are extremely soft. Hence the cylinders fluctuate significantly about their ideal trigonal lattice positions. However, we can run the small systems long enough to get an idea of the average radius of the cylinders. Using this average radius, we can construct a larger system in which cylinders of roughly the same radius are positioned on ideal trigonal lattice sites. This is what we used as an initial configuration. The system is then run for long times (30,000 $\tau$) while we track the center of mass of each cylinder. The system we used contained 1776 polymers of length 10. The simulation with constant strain parallel to the fluid direction and constant pressure parallel to the two solid directions averaged to $80.9363 \times 69.9274 \times 3.87169$. This allowed us to have 64 cylinders in the simulation cell and eleven distinct phonons on the path in reciprocal space shown in Figure 3(c).

## 3.3 Reorientation under shear

When diblock copolymer melts in the lamellar phase are subjected to shear flow they reorient to the parallel or perpendicular phase, depending on shear rate [48, 49], as illustrated in Fig. 6. This can also be seen in molecular dynamics simulations [11, 12, 13] where the qualitative results found in experimental studies can be reproduced.

We are able to see some of this preferential orientation based on shear rate with our model.

Starting from a transverse orientation of the lamellar phase and imposing a constant shear rate on the system, we can begin to address what shear rates send the system into parallel and perpendicular alignments. It has been suggested experimentally [50, 51, 52, 53] and theoretically [11] that low shear rates should align the system in the parallel alignment while high shear rates select the perpendicular alignment. However to do so requires careful consideration of the geometry of the simulation box as the lamellae realign.

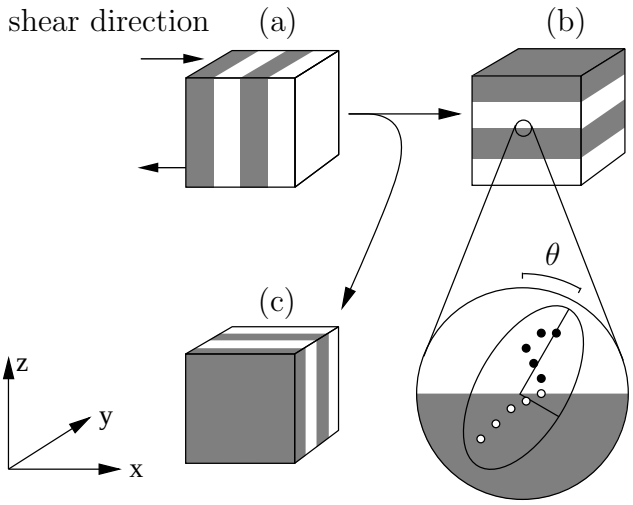


Figure 6: Shearing from the transverse (a), to parallel (b), or perpendicular (c), alignments. The coordinate system denotes the Cartesian coordinate system used in the following text and figures.

Under shear flow, the polymers are trying to minimize the energy and entropy production associated with the phase they are found in. The lamellar phase minimizes the energy by minimizing the interfacial area between $A$ and $B$ monomers. It then orients with respect to the shear flow such that one fluid direction is aligned with the shear flow. We fixed the size of the simulation box in the direction of shear flow so this does not pose a problem. If we did not, the system will shrink and become two-dimensional.

Even when the box geometry is allowed to fluctuate, it is possible that the systems finds itself trapped with diagonally oriented lamellae. However, a diagonal orientation is not expected to be the final equilibrium state. We have seen this for a particular simulation initiated from the transverse phase, and sheared at a moderate rate of $0.04\tau^{-1}$. We expect to see the lamellae reorient into either the parallel or perpendicular phase. However, they align with the lamellae oriented in the shear direction and diagonally between the perpendicular and parallel phases.

This orientation is a local energy minimum that is found when the simulation box does not change to the proper spacing quickly enough as the reoriented lamellar phase is emerging. Once the diagonal phase is found, there is a very high energy barrier to reorientation. The lamellae cannot simply rotate. If you consider the periodic boundary conditions, it is easy to see the two lamellae in figure 7 are actually part of a single lamellae. Reorientation would therefore require breaking this domain and rotating the pieces into a vertical or horizontal alignment where they

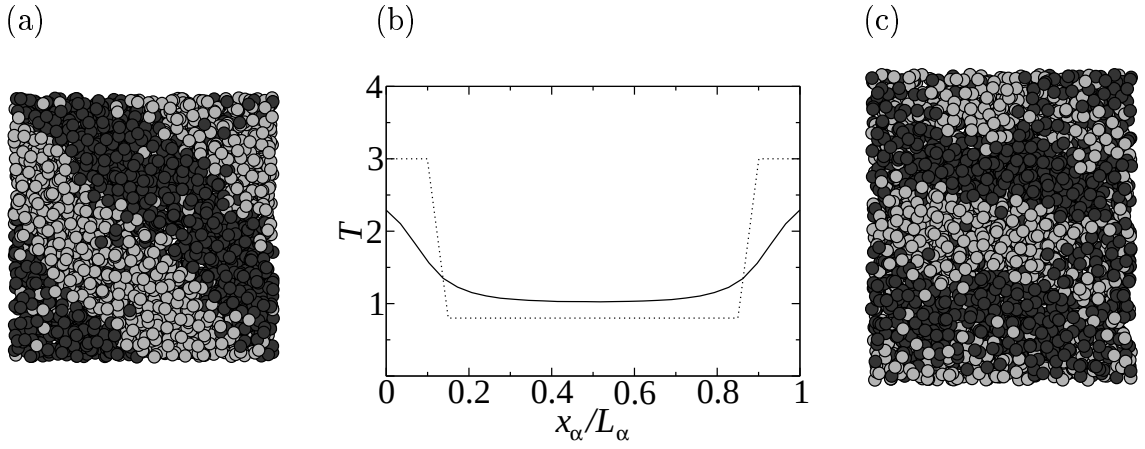


Figure 7: Left: Simulation stuck in diagonal phase. The graph is a view on the $y-z$ plane. Middle: Imposed temperature profile to allow for reorientation. $x_\alpha$, with $\alpha = 2, 3$, represents either $y$ or $z$ direction. Right: Reoriented parallel phase. The lamellae are more disordered near the edges due to the higher temperature there. Simulation parameters are the same as those for Fig. 2.

would form two separate lamellae. This energy barrier is exceedingly unlikely to be passed in any amount of simulation time.

To overcome the energy barrier involved in breaking the lamellae, when the lamellae orient diagonally in our simulations, we increase the temperature near the boundaries of the simulation box, melting the phase around the edges while imposing the system to the same shear rate. This type of boundary layer has been used effectively in studies of incommensurate systems with similar symmetry constraints [54]. The imposed and measured temperatures across the $x$ dimension of the simulation box are shown in figure 7(b). Near the edges, we ensure that the measured temperature is greater than $T^*$, while away from the edges, the temperature is fixed below $T^*$. This melting breaks the lamellae within the hot regions, and allows the remainder to rotate freely into a preferable alignment as shown in Fig. 7(c).

In the following simulations we actually fixed the box size in all directions based on an equilibrated equilibrium box size. This was not necessary and, in principle undesirable, however it should not have a qualitative effect on the results found. We will investigate the effect of relaxing this assumption in future work.

We now investigate the molecular origin of the realignment. The transverse phase is not stable under shear because it has solid properties along the shear direction (cf. the discussion surrounding Fig. 2) and hence is incompatible with a steady-state flow velocity perpendicular to the lamella. That leaves both the parallel and perpendicular alignments (Fig. 6) as possible steady state configurations. To see which one is favorable, it is worthwhile to examine the state of individual polymers.

When homopolymers are subjected to shear, they are stretched and start to show orientational preferences [55]. That is, rather than the monomers being, on average, distributed in a spherically symmetric distribution about the center of mass, the distribution becomes el-

lipsoidal. The principal axes of the ellipsoid then tends to have a preferred orientation with respect to the shear velocity, in a manner analogous to the way that liquid crystals orient with respect to shear. Our block copolymer melts already have non-spherical distributions due to the phase separation (e.g. the $A$ end will always be on the $A$ side of the lamellae and the $B$ end will always be on the $B$ side). As such, even low shear rates should drive the reorientation.

We can calculate the orientational preference of the polymers by considering average shape and orientation of the ellipse that the monomers of each polymer are likely to be found in. To do so, we calculate the tensor of gyration for each polymer in the simulation box, at each time step, by locating the center of mass of each polymer, $(x_c, y_c, z_c)$ and finding the average

$$\mathbf{G}_{\alpha\beta} = \langle(\alpha_i - \alpha_c)(\beta_i - \beta_c)\rangle \tag{17}$$

where $\alpha_i, \beta_i \in \{x_i, y_i, z_i\}$ are the coordinates of each monomer in the polymer chain. The eigenvectors of the orientation matrix give the major and minor axes of the ellipse that, on average, describes the polymers. The eigenvalues of this matrix give the squared axis length in each of the three directions.

As we found from the soft boundary simulations described above, the system prefers the parallel phase at low shear rates. This is entirely analogous to liquid crystals, where for low shear rates the polymers should orient in the shear plane with a fixed average angle with respect to the shear velocity, favoring the parallel state. In a uniaxial system, which describes the equilibrium configuration of the molecules with one major axis and two equal minor axes (see Fig.8(a)), the molecules are unstable to fluctuations of the major axes out of the shear plane (defined by shear velocity and the shear gradient direction). This is because any fluctuation of the major axis out of the shear plane will result in the ends or the polymer experiencing different flow velocities which should bring it back into shear plane.

Figure 9 shows the orientation of the major axes or the tensor of gyration as a function of shear rate. The angle the major axes makes into the shear flow $\theta$ is defined in Fig. 6(b). At low shear rates, the polymers are oriented perpendicular to the lamella and perpendicular to the flow velocity. As the shear is increased, the molecules start to align towards the flow velocity, but remain in the shear plane. The angle reflects the balance of the structural force trying to align the polymer perpendicular to the lamella and the force trying to align it along the shear flow. As long as the structural force is dominant the parallel phase is stable. The parallel phase becomes unstable when the angle exceeds 45°, as is evident in Fig. 9.

The details of this transition can be elucidated quantitatively by making use of the liquid crystal analogy. Once steady state is reached, the shear flow is described by a velocity field $\mathbf{v} = (\dot{\gamma}z, 0, 0)$. If we take the director $\mathbf{n}$ to be the unit vector coincident with the eigenvector associated with the largest eigenvalue of $\mathbf{G}$, then if $\mathbf{n}$ is in the shear plane it can be described by $\mathbf{n} = (\sin\theta, 0, \cos\theta)$. The unit normal to the lamella in the parallel state is $\mathbf{k} = (0, 0, 1)$. The viscous torque density is then [56, 57]

$$\Gamma^v = \gamma_1 \mathbf{n} \times [-\dot{\mathbf{n}} + (\lambda\mathbf{D} - \mathbf{\Omega}) \cdot \mathbf{n}], \tag{18}$$

where $\mathbf{D} = (\mathbf{W} + \mathbf{W}^T)/2$ and $\mathbf{\Omega} = (\mathbf{W} - \mathbf{W}^T)/2$ are the symmetric part and the anti-symmetric part respectively of the velocity gradient tensor $W_{\alpha\beta} = \partial_\beta u_\alpha$. $\gamma_1$ is a viscosity and $\lambda$

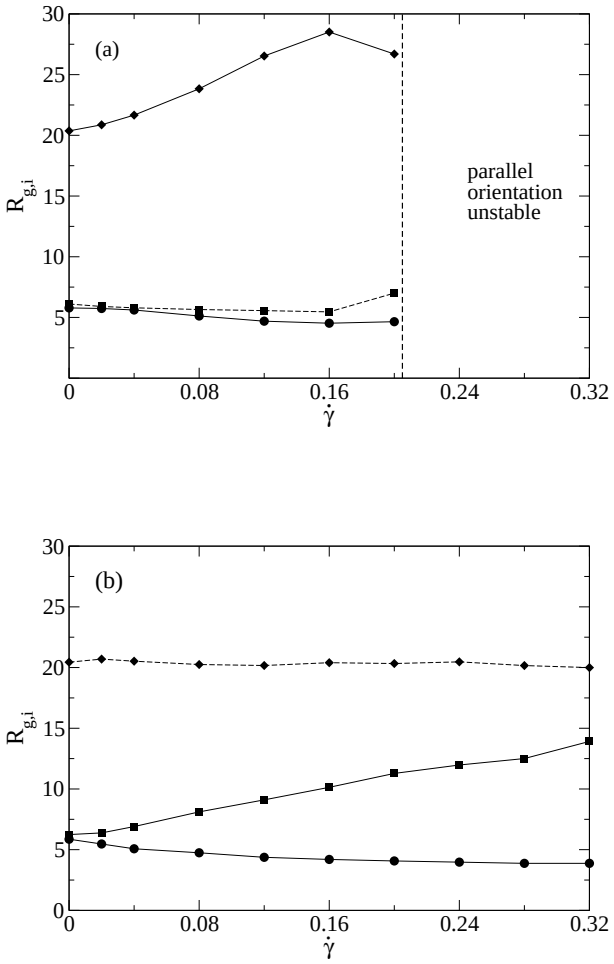


Figure 8: (a) Eigenvalues $R_{\mathrm{g},i}$ of the orientation matrix in parallel configuration. (b) Eigenvalues $R_{g,i}$ of the orientation matrix in the perpendicular configuration. Note that in contrast to (a), polymers are biaxial in (b) and are becoming more and more disk-like as the shear rate increases. In both graphs, $R_{yy}$ is an eigenvalue, which is represented as a dotted line. Same details as in Fig. 2.

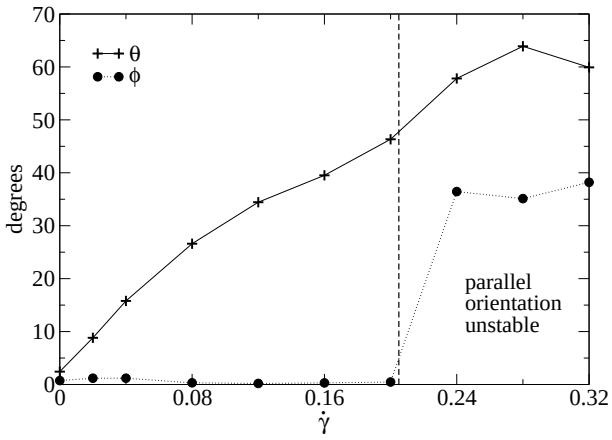


Figure 9: Angle into the shear flow $\theta$, in the parallel configuration (+) and the angle $\Phi$ perpendicular to shear flow (•).

is a dimensionless ratio of viscosities related to the relative magnitude of the rotational ($\mathbf{\Omega}$) to the aligning ($\mathbf{D}$) flow effects[56, 57]. In addition to the viscous torque, there is a torque due to the "crystal field" created by the lamella themselves. If we assume this field acts in the same way as a magnetic or electric field (namely to align the director along the field) of magnitude $b\mathbf{k}$, then this produces an an additional torque density of [56]

$$\Gamma^c = b(\mathbf{n}\cdot\mathbf{k})\mathbf{n}\times\mathbf{k}. \tag{19}$$

Steady state configurations require that $\Gamma^v + \Gamma^c = 0$. For our case, the total torque along the $y$-axis gives the equation

$$\gamma_1\dot{\gamma}(1+\lambda\cos 2\theta) - b\sin 2\theta = 0. \tag{20}$$

For $0 \le \theta \le \pi/2$, $\sin 2\theta = \sqrt{1-\cos^2 2\theta}$ and Eq.(20) becomes an easily solved quadratic equation for $\cos 2\theta$. However, the possible stable alignment angles are restricted to $0 \le \theta \le \pi/4$ as a consequence of the equation being for $\cos 2\theta$ rather than $\cos\theta$.

At high shear rates, the polymers orient out of plane into the perpendicular configuration. As we mentioned above, for rod-like molecules this phase is not stable. Indeed in liquid crystal systems this phase is accompanied by the minor axes rotating continuously in a "kayaking" or "log-rolling" phase [58] (The $\dot{\mathbf{n}}$ term in Eq.(18) is required to obtain a solution). However, our polymer molecules have more degrees of freedom and are able to accommodate the perpendicular configuration by becoming biaxial, or disk-like. This can be seen in Fig. 8(b).

# 4 Conclusions

The use of molecular dynamics in the study of diblock copolymer systems has been somewhat limited. Some of the limitations are related to experimental details, such as polymer lengths consisting of thousands of monomers, that cannot in the foreseeable future be realized in computer simulations. However, as can be seen by our simulations, and others [11, 12, 13, 14, 15],

much of the qualitative behavior of the systems we can simulate is identical to that of experimental systems. Thus, molecular dynamics can reveal many of the underlying microscopic mechanisms for macroscopic behavior such as the shear induced molecular orientation driving the transition from the parallel to perpendicular configuration for lamella. These local mechanisms may also provide the driving force for shear alignment of polycrystalline samples, however, to investigate this fully, grain boundary motion would have to be studied.

In our study, we found it necessary to adjust the potentials to ensure phase separation for short chains. Further, as simulations are typically done with periodic boundary conditions, it is essential to understand and allow for commensurability of the underlying microstructure with the periodic simulation box. When the underlying microstucture rotates, it may be necessary to have a "soft" boundary layer where the system is heated above the critical point to avoid traps and mobius strip type configurations.

Once these technical issues are properly dealt with molecular dynamics can be used to parameterize simpler theories such as particle plus field type models for the microstructure. For the hexagonal phase we found that simple harmonic two-body potentials cannot reproduce the elastic properties in the form of the phonon spectrum. However, in future work we plan on investigating this further and see if additional terms, such as three-body forces can overcome these problems.

In the shear aligned lamella, we found that reorientation is driven by alignment of the polymers with the shear flow. An analogy to similar phenomena in liquid crystals appears to give a satisfying model for the effect. In future work we plan on examining this further, parameterizing the viscous and crystal torques to get a more quantitative comparison.

**Acknowledgments.** We thank An-Chan Shi for helpful discussions. We thank NSERC for financial support and Sharcnet for computational resources.

# References

[1] K. Binder. Phase transitions of polymer blends and block copolymer melts in thin films. *Adv. Polymer Science*, 138:1–89, 1999.

[2] J. Baschnagel et al. Bridging the gap between atomistic and coarse-grained models of polymers: Status and perspectives. *Adv. Polymer Science*, 152(41-156), 2000.

[3] G.S. Grest, M.-D. Lacasse, K. Kremer, and A.M. Gupta. Efficient continuum model for simulating polymer blends and copolymers. *J. Chem. Phys.*, 105(23):10583–10594, 1996.

[4] T. Soddemann, B. Dünweg, and K. Kremer. A generic computer model for amphiphilic systems. *Eur. Phys. J. E*, 6(5):409–419, 2001.

[5] M. Kröger, W. Loose, and S. Hess. Rheology and structural changes of polymer melts via nonequilibrium molecular-dynamics. *J. Rheol.*, 37:1057–1079, 1993.

[6] M. Kröger and S. Hess. Rheological evidence for a dynamical crossover in polymer melts via nonequilibrium molecular dynamics. *Phys. Rev. Lett.*, 85:1128–1131, 2000.

[7] R. Khare, J.J. dePablo, and A. Yethiraj. Rheology of confined polymer melts. *Macromolecules*, 29:7910–7918, 1996.

[8] M.J. Stevens et al. Comparison of shear flow of hexadecane in a confined geometry and in bulk. *J. Chem. Phys.*, 106:7303–7314, 1997.

[9] G.S. Grest. Polymers in confined environments. *Adv. Polymer Science*, 138:149–183, 1999.

[10] T. Kreer, M.H. Müser, K. Binder, and J. Klein J. Frictional drag mechanisms between polymer-bearing surfaces. *Langmuir*, 17:7804–7813, 2001.

[11] H. Guo, K. Kremer, and T. Soddemann. Nonequilibrium molecular dynamics simulation of shear-induced alignment of amphiphilic model systems. *Phys. Rev. E*, 66(6):Art. No. 061503, 2002.

[12] H. Guo and K. Kremer. Molecular dynamics simulation of the phase behavior of lamellar amphiphilic model systems. *J. Chem. Phys.*, 119(17):9308–9320, 2003.

[13] T. Soddemann, G.K. Auernhammer, H. Guo, B. Dünweg, and K. Kremer. Shear-induced undulation of smectic-a: Molecular dymamics simulations vs. analytical theory. *Euro. Phys. J. E*, 13(2):141–151, 2004.

[14] I. Rychkov and K. Yoshikawa. Structural changes in block copolymer solutions under shear flow as determined by non-equilibrium molecular dynamics. *Macromol. Theory Simul.*, 13:257–264, 2004.

[15] I. Rychkov and K. Yoshikawa. Nonlinear rheological behavior associated with structural transitions in block copolymer solutions via nonequilibrium molecular dynamics. *J. Chem. Phys.*, 120:3482–3488, 2004.

[16] F.S. Bates. Block copolymers - designer soft materials. *Phys. Today*, 52:32, 1999.

[17] I.W. Hamley. *The Friction and Lubrication of Solids*. Oxford University Press, London, 1999.

[18] M.W. Matzen and F.S. Bates. Unifying weak- and strong-segregation block copolymer theories. *Macromolecules*, 29(4):1091–1098, 1996.

[19] L. Leibler. *Macromolecules*, 13:1602, 1980.

[20] M.W. Matsen and M. Schick. *Phys. Rev. Lett.*, 72:2660, 1994.

[21] M.W. Matsen. *J. Phys.: Condens. Matter*, 14:R21, 2002.

[22] M.S. Turner, M. Rubinstein, and C.M. Marques. *Macromolecules*, 27:4986, 1994.

[23] F.S. Bates G.H. Fredrickson. Dynamics of block copolymers: Theory and experiment. *Annual Review of Materials Science*, 26:501–550, 1996.

[24] R.H. Colby. Block copolymer dynamics. *Current opinion in colloid and interface science*, 1(4):454–465, 1996.

[25] I.W. Hamley. Structure and flow behaviour of block copolymers. *J. Phys.: Cond. Matt.*, 13:R643–R671, 1999.

[26] Z. F. Huang, F. Drolet, and J. Vinals. Motion of a transverse/parallel grain boundary in a block copolymer under oscillatory shear flow. *Macromolecules*, 36:9622–9630, 2003.

[27] S. Stangler and V. Abetz. Orientation behavior of ab and abc block copolymers under large amplitude oscillatory shear flow. *Rheologica Acta*, 42(6):569–577, 2003.

[28] A.V.M. Zvelindovsky and G.J.A. Sevink. Sphere morphology of block copolymer systems under shear. *Europhys. Lett.*, 62(3):370–376, 2003.

[29] M.E. Cates and S.T. Milner. Role of shear in the isotropic-to-lamellar transition. *Phys. Rev. Lett.*, 62:1856–1859, 1989.

[30] A.-C. Shi. *J.Phys.: Condens. Matter*, 11:10183, 1999.

[31] S.A. Brazovskii. *Sov. Phys. JETP*, 41:85, 1975.

[32] E.I. Kats, V.V. Lebedev, and A.R. Muratov. *Phys. Rep.*, 228:1, 1993.

[33] T.Ohta and K. Kawasaki. *Macromolecules*, 19:2621, 1986.

[34] Z.-G. Wang R.A. Wickham, A.-C. Shi. *J. Chem. Phys.*, 118:10293, 2003.

[35] M.J. Stevens and M. O. Robbins. Simulations of shear-induced melitng and ordering. *Phys. Rev. E*, 48:3778–3792, 1993.

[36] K. Zahn, A. Wille, G. Maret, S. Sengupta, and P. Nielaba. Elastic properties of 2d colloidal crystals from video microscopy. *Phys. Rev. Lett.*, 90(15):Art. No. 155506, 2003.

[37] M.P. Allen and D.J. Tildesley. *Computer Simulation of Liquids*. Clarendon Press, Oxford, 1987.

[38] T. Soddemann, B. Dünweg, and K. Kremer. Dissipative particledynamics: A useful thermostat for equilibrium and nonequilibrium molecular dynamics simulations. *Phys. Rev. E*, 68(4):Art. No. 046702, 2003.

[39] A.W. Lees and S.F. Edwards. The computer study of transport processes under extreme conditions. *J. Phys. C*, 5(15):1921–1929, 1972.

[40] M. Murat, G.S. Grest, and K. Kremer. Statics and dynamics of symmetric diblock copolymers: A molecular dynamics study. *Macromolecules*, 32(3):595–609, 1999.

[41] D. Ehlich, M. Takenaka, S. Okamoto, and T. Hashimoto. *Macromolecules*, 26:189–197, 1993.

[42] H. Kodama and M. Doi. Shear-induced instability of the lamellar phase of a block copolymer. *Macromolecules*, 29:2652, 1996.

[43] M. W. Hamersky, M. Tirrell, and T. P. Lodge. Anisotropy of diffusion in a lamellar styrene-isoprene block copolymer. *Langmuir*, 14:6974, 1998.

[44] S. Sengupta, P. Nielaba, M. Rao, and K. Binder. Elastic constants from microscopic strain fluctuations. *Phys. Rev. E*, 61(2):1072–1080, 2000.

[45] L.W. Bruch. Elasticity of a quantum monolayer solid. *Phys. Rev. B*, 45:7161–7164, 1991.

[46] P. Schöffel and M.H. Müser. Elastic constants of quantum solids by path integral simulations. *Phys. Rev. B*, 63:Art. No. 224108, 2001.

[47] M.R. Hammond et al. Adjustment of block copolymer nanodomain sizes at lattice defect sites. *Macromolecules*, 36(23):8712–8716, 2003.

[48] F. Drolet, P. Chen, and J. Viñals. Lamellae alignment by shear flow in a model of diblock copolymers. *Macromolecules*, 32(25):8603–8610, 1999.

[49] P. Chen and J. Viñals. Lamellar phase stability in diblock copolymers under oscillatory shear flows. *Macromolecules*, 35(10):4183–4192, 2002.

[50] N.P. Balsara and B. Hammouda. Shear effects on solvated block-copolymer lamellae - polystyrene-polyisoprene in dioctyl phthalate. *Phys. Rev. Lett.*, 73:360, 1994.

[51] Y. M. Zhang, U. Wiesner, and H. W. Spiedd. Frequency-dependence of orientation in dynamically sheared diblocj copolymers. *Macromolecules*, 28:778, 1995.

[52] I. W. Hemley. The effect of shear on ordered block copolymer solutions. *Curr. opin. colloid. in.*, 5:342, 2000.

[53] A. N. Morozov and J. G. E. M. Fraaije. Orientations of the lamellar phase of block copolymer melts under oscillatory shear flow. *Phys. Rev. E*, 65:Art. No. 031803, 2002.

[54] C. Denniston and C. Tang. Incommensurability in the frustrated two-dimensional xy model. *Phys. Rev. B*, 60:3163–3168, 1999.

[55] A. Onuki. Phase transitions of fluids in shear flow. *J.Phys.: Condens. Matter*, 9:6119–6157, 1997.

[56] P.G. de Gennes and J. Prost. *The Physics of Liquid Crystals, 2nd ed.* Clarendon Press, Oxford, 1993.

[57] A.D. Rey and M.M. Denn. Dynamical phenomena in liquid-crystalline materials. *Ann. Rev. Fluid Mech.*, 34:233–66, 2002.

[58] T. Tsuji and A. D. Rey. Orientation mode selection mechanisms for sheared nematic liquid crystalline materials. *Phys. Rev. E*, 57:5609–5625, 1998.